

Supramolecular dioxygen receptors composed of an anionic water-soluble porphinatoiron(II) and cyclodextrin dimers†

Koji Kano,* Syoichi Chimoto, Mariko Tamaki, Yoshiki Itoh and Hiroaki Kitagishi

Received 25th August 2011, Accepted 20th September 2011

DOI: 10.1039/c1dt11596k

Three types of per-*O*-methylated β -cyclodextrin dimers, Im2CD, Im3NHCD and Py3NHCD, were prepared as globin models. Im2CD was synthesized by the condensation reaction of mono(2^A-amino)-per-*O*-methylated β -cyclodextrin with 3-(1*H*-imidazol-1-yl)pentanedioic acid. Im3NHCD and Py3NHCD were obtained through the S_N2 reactions of mono(2^A,3^A-epoxy)-per-*O*-methylated β -cyclodextrin with 3-(1*H*-imidazol-1-yl)pentane-1,5-diamine and 3,5-bis(aminomethyl)pyridine, respectively. These cyclodextrin dimers formed 1 : 1 supramolecular inclusion complexes of tetrakis(4-sulfonatophenyl)porphinatoiron(II) (Fe^{II}TPPS) in aqueous solution. The supramolecular complexes bound dioxygen (O₂), with the O₂ affinity of the Fe^{II}TPPS/Im3NHCD complex ($P_{1/2}^{O_2} = 1.5 \pm 0.1$ Torr) being much higher than those of the Fe^{II}TPPS/Im2CD (36 ± 2 Torr) and Fe^{II}TPPS/Py3NHCD complexes (70 ± 5 Torr). On the basis of the results of the present study and previous results, it is concluded that the imidazole axial ligand at the linker attached at the 3- and 3'-positions of the cyclodextrin units causes higher O₂ affinity as compared with the imidazole ligand at the 2- and 2'-positions and the pyridine ligand at the 2,2'- or 3,3'-positions. The electron donating ability and orientation of the axial ligand may control the O₂ affinity of a supramolecular receptor.

Introduction

Haemoglobin (Hb) and myoglobin (Mb) are dioxygen (O₂) transport and storage proteins, respectively, which are composed of iron protoporphyrin IX and a protein, globin. For transferring dioxygen from oxyHb in blood to deoxyMb in muscle, the dioxygen affinity of human Mb ($P_{1/2} = 0.69$ Torr)¹ is much higher than that of human Hb in a tense (T) state (26 Torr).² The dioxygen affinity of Hb is artfully controlled by the conformational change of this heme protein tetramer.^{3–5} To release the dioxygen of oxyHb in muscle, interactions between the heme proteins become tight to form a T state, resulting in lowering the dioxygen affinity. Leghemoglobin (Lb) is a monomeric heme protein that binds dioxygen and therefore belongs to the Mb family. Lb is located at the root nodules of leguminous plants to provide anaerobic conditions around the root nodules. The dioxygen affinity of soybean Lb ($P_{1/2} = 0.04$ Torr) is about 18 times higher than that of Mb (0.7 Torr).⁶ Single-crystal X-ray analysis indicates that the plane of the proximal histidine (His) of Mb completely aligns with a line connecting the nitrogen atom of a pyrrole with that of an opposite pyrrole (eclipsed conformation),⁷ while the plane of the proximal His of Lb crosses that line (staggered conformation).⁸ The orientation of the axial His may control the

O₂ affinity of the heme protein. Although a large number of studies on proximal ligand effects have been carried out with respect to natural and mutated heme proteins,^{9–14} the detailed mechanism for controlling the O₂ affinity in a biological system has not been clarified definitely.

The modelling of Hb and Mb has been an attractive research subject. Many sophisticated Hb/Mb models have been prepared to clarify the detailed mechanism for dioxygen binding to an iron centre of a heme protein.^{2,15} Until recently, however, no good functional model of globin surrounding iron protoporphyrin IX had been presented. Therefore, so far, a Hb/Mb model that functions in an aqueous solution has not been proposed. Globin provides a hydrophobic environment to exclude free water molecules from the porphyrin centre, to which a proximal His coordinates to donate electrons to the Fe–O₂ bond. A distal His is not essential for the formation of the dioxygen adduct of the heme protein, although it greatly stabilizes the dioxygen adduct through hydrogen bonding between the bound dioxygen and the distal His.^{16–19} In short, a globin model is required to provide an electron-donative axial ligand and a hydrophobic environment to a ferrous porphyrin. As globin models that satisfy these requirements, we have previously prepared per-*O*-methylated β -cyclodextrin dimers such as Py3CD,^{20,21} Py2CD²² and Im3CD²³ (Fig. 1), which include tetrakis(4-sulfonatophenyl)porphinatoiron(II) (Fe^{II}TPPS) to form the Fe^{II}TPPS/Py3CD (hemoCD1), Fe^{II}TPPS/Py2CD (hemoCD2) and Fe^{II}TPPS/Im3CD 1 : 1 inclusion complexes, respectively. These supramolecular complexes satisfy the minimum requirements for use as Hb/Mb models and therefore bind

Department of Molecular Chemistry and Biochemistry, Doshisha University, Tatara, Kyotanabe, Kyoto 610-0321, Japan. E-mail: kkanoo@mail.doshisha.ac.jp; Fax: +81 774 65 6845; Tel: +81 774 65 6624

† Electronic supplementary information (ESI) available. See DOI: 10.1039/c1dt11596k

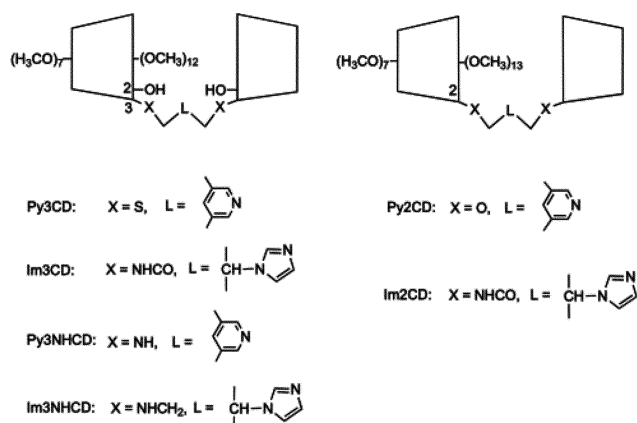


Fig. 1 Structures of per-*O*-methylated β -cyclodextrins as heme protein models.

dioxygen in aqueous solution.^{20–23} The dioxygen affinity of an O₂-receptor is commonly evaluated by the $P_{1/2}$ value, which corresponds to the partial dioxygen pressure at which half of the receptor molecules are oxygenated. The $P_{1/2}$ values of hemoCD1, hemoCD2 and the Fe^{II}TPPS/Im3CD complex are 10,²⁴ 176²² and 1.7 Torr,²³ respectively, at pH 7.0 and 25 °C. Recently, the $P_{1/2}$ value for hemoCD1 was corrected and established as 10 Torr.²⁴ It is interesting that each model O₂ receptor shows different O₂ affinity. However, the number of model systems is too small to deduce a general conclusion on factor(s) that controls the O₂ affinity. In this study, we synthesized an additional three supramolecular O₂ receptors (Fe^{II}TPPS complexes of Im2CD, Im3NHCD and Py3NHCD, Fig. 1) and studied their O₂ affinities. We expected to know the relationship between the structures of the cyclodextrin dimers as the globin models and the O₂ affinities of their Fe^{II}TPPS complexes.

Experimental

Materials

Fe^{III}TPPS was prepared according to the procedures described in the previous papers.²⁵ Py3CD,^{20,21} Py2CD,²² and Im3CD²³ used in this study were the same as those described in previous studies. The synthesis of mono(2^A,3^A-epoxy)-hexakis(2^B,2^C,2^D,2^E,2^F,2^G-*O*-methyl)-hexakis(3^B,3^C,3^D,3^E,3^F,3^G-*O*-methyl)-heptakis(6-*O*-methyl)- β -cyclodextrin (2,3-EpoPMeCD) was described in a previous paper.²⁰ 3,5-Bis(chloromethyl)pyridine,²⁶ 3-(1*H*-imidazol-1-yl)pentane-1,5-diamine,²⁷ 3-(1*H*-imidazol-1-yl)pentanedioic acid,²⁸ and mono(2^A-amino)-hexakis(2^B,2^C,2^D,2^E,2^F,2^G-*O*-methyl)-heptakis(3-*O*-methyl)-heptakis(6-*O*-methyl)- β -cyclodextrin (2-NH₂PMeCD)²⁹ were synthesized according to the procedures reported in the literature. The synthetic procedures for Py3NHCD, Im3NHCD and Im2CD are shown below. Other chemicals were purchased and used as received. Water was purified using a Millipore Simpax 1. Pure O₂ (99.999%), pure N₂ (99.999%), and CO (> 99.9%) gases were purchased from Sumitomo Seika Chemicals.

3,5-Bis(phthalimide methyl)pyridine

A mixture of 3,5-bis(chloromethyl)pyridine (1.15 g, 6.53 mmol) and potassium phthalimide (2.42 g, 13.1 mmol) in DMF (16 mL)

was stirred at 140 °C for 5 h. After evaporating the solvent, the residue was purified by silica gel column chromatography with chloroform and ethyl acetate to afford a colourless solid (1.95 g, 75%). ¹H NMR (400 MHz, CDCl₃, TMS) δ 8.61 (s, 2H), 7.83–7.88 (m, 5H), 7.70–7.75 (m, 4H), 4.84 (s, 4H); *m/z* (FAB, *m*-NBA) 398 (calcd for [M+H]⁺: 398.12).

3,5-Bis(aminomethyl)pyridine trihydrobromide

A solution of 3,5-bis(phthalimide methyl)pyridine (0.3 g, 0.75 mmol) in 50% hydrobromic acid (4.5 mL) was refluxed for 5 h. The precipitates were removed by filtration and the filtrate was evaporated. The solid thus obtained was washed with ethanol (7 mL). Yield: 88%, ¹H NMR (400 MHz, DMSO-d₆, TMS) δ 8.91 (s, 2H), 8.49 (s, 6H), 8.39 (s, 1H), 4.22 (q, 4H).

Py3NHCD

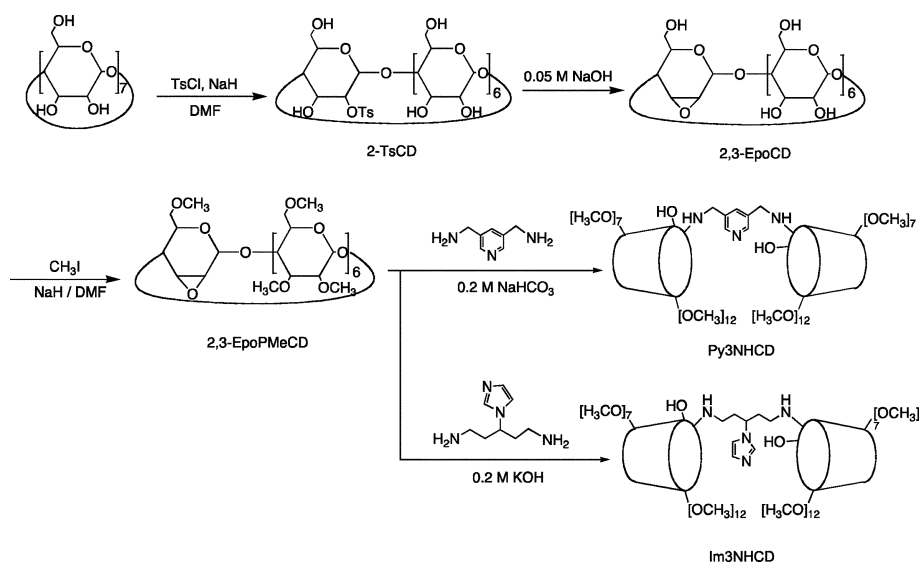
A mixture of 3,5-bis(aminomethyl)pyridine trihydrobromide (0.1 g, 0.26 mmol) and 2,3-EpoPMeCD (1.0 g, 0.72 mmol) in 0.2 M aqueous sodium hydrogen carbonate (35 mL) was refluxed overnight under an argon atmosphere. After the reaction, the reaction mixture was extracted with dichloromethane (2 × 80 mL). After drying on Na₂SO₄, dichloromethane was evaporated and the residue was purified by silica gel column chromatography with chloroform/acetone (5/3) → chloroform/acetone/methanol (12/7/1) → chloroform/methanol (10/1) to obtain a colourless solid (0.18 g, 0.062 mmol, 17%). ¹H NMR (400 MHz, CDCl₃, TMS) δ 8.90 (s, 2H), 8.61 (s, 1H); Anal. calcd for C₁₂₉H₂₂₃O₆₈N₃·2H₂O·CHCl₃: C 51.03, H 7.51, O 36.61, N 1.37. Found: C 51.11, H 7.49, O 37.97, N 1.31%.

Im3NHCD

A mixture of 3,5-bis(aminomethyl)pyridine trihydrobromide (0.1 g, 0.26 mmol) and 2,3-EpoPMeCD (1.20 g, 0.87 mmol) in 0.2 M aqueous sodium hydrogen carbonate (42 mL) was refluxed overnight under an argon atmosphere. After the reaction, the reaction mixture was extracted with chloroform (2 × 80 mL). After drying on Na₂SO₄, chloroform was evaporated and the residue was purified by silica gel column chromatography with chloroform/acetone (5/3) → chloroform → chloroform/methanol (10/1) to obtain a colourless solid (0.12 g, 9%). ¹H NMR (400 MHz, CDCl₃, TMS) δ 7.56 (s, 1H), 7.08 (s, 1H), 6.96 (s, 1H), 5.06–5.32 (m, 14H), 3.89–3.23 (m, 251H), 3.15–3.20 (m, 15H), 2.64 (d, 1H), 2.35 (s, 3H), 1.97 (s, 3H); *m/z* (MALDI TOF, α -CHCA) 2955 (calcd for [M+Na]⁺: 2956.46). Anal. calcd for C₁₃₀H₂₂₈O₆₈N₄·H₂O: C 53.20, H 7.83, O 37.07, N 1.91. Found: C 52.87, H 7.85, O 37.38, N 1.90%.

Im2CD

A mixture of 3-(1*H*-imidazol-1-yl)pentanedioic acid (6 mg, 0.026 mmol), 1-hydroxybenzotriazole (HOBT, 17 mg, 0.11 mmol) and *N,N'*-dicyclohexylcarbodiimide (DCC, 23 mg, 0.11 mmol) in DMF (5 mL) was stirred at room temperature for 14 h. After the green–yellow colour of the reaction mixture disappeared, 2-NH₂PMeCD (150 mg, 0.11 mmol) was added into the activated dicarboxylic acid solution. The reaction mixture was further stirred at room temperature for 14 h. After the reaction, the solvent



Scheme 1 Synthesis of Py3NHCD and Im3NHCD.

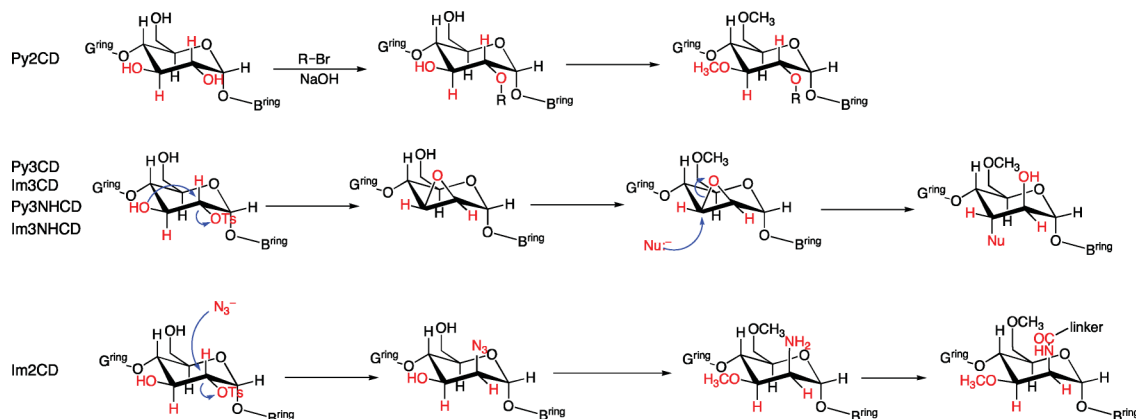


Fig. 2 Alteration in stereochemistry during the preparation of the CD dimers.

was removed *in vacuo* and the residue was purified by silica gel column chromatography with chloroform/methanol (10/1) and gel permeation chromatography with methanol. Yield; 46%, ^1H NMR (400 MHz, CDCl_3 , TMS) δ 7.65 (*s*, 1H), 7.03 (*d*, 1H), 6.92 (*d*, 1H), 4.96–5.17 (*m*, 12H), 3.33–3.99 (*m*, 206H), 3.18–3.25 (*m*, 15H). Anal. calcd for $\text{C}_{132}\text{H}_{228}\text{O}_{70}\text{N}_4\cdot 4\text{H}_2\text{O}$: C 51.76, H 7.77, O 38.64, N 1.83. Found: C 51.64, H 7.53, O 38.92, N 1.91%.

Measurements

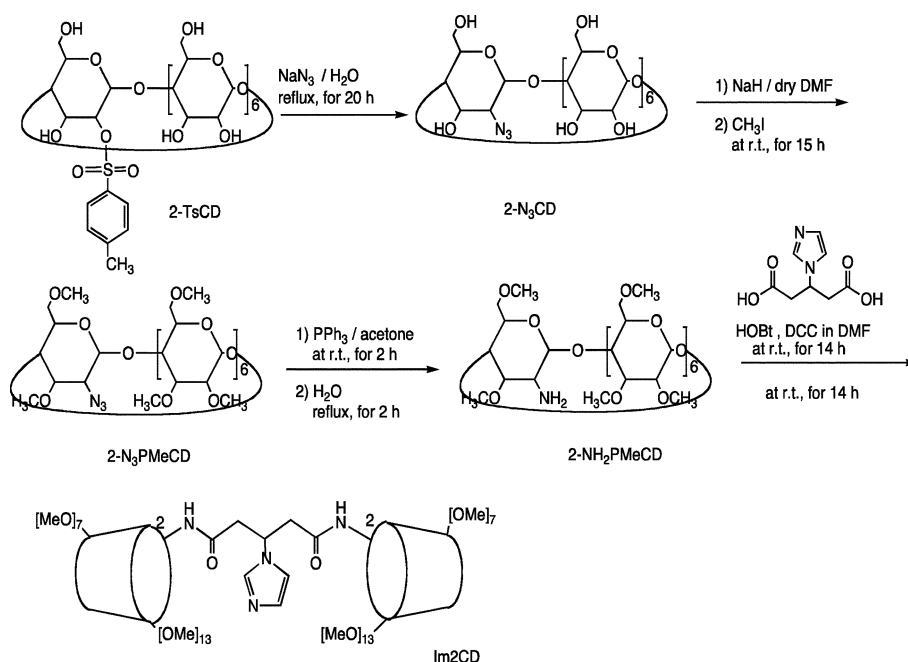
UV-vis spectra were taken using Shimadzu UV-2100 and UV-2450 spectrophotometers with thermostatic cell holders. The pH values were measured with a Horiba pH meter M-12. ^1H NMR spectra were taken using a JEOL JNM-A400 spectrometer (400 MHz). TMS (Nacalai) was used as an internal standard. FAB MS spectra were recorded on a JEOL JMS-700 spectrometer. MALDI-TOF MS measurements were performed using a Shimadzu KOMPACT MALDI IV spectrometer. Mixed O_2 gases with various partial pressures in N_2 were prepared with a KOFLOC GM-4B gas mixing apparatus (Kyoto, Japan). Molecular mechanics calculations were performed using CONFLEX/MM3 (extensive search) parameters in the Scigress version 2.2.1 software program (Fujitsu, Japan).

Results and discussion

Synthesis of globin models

The synthetic routes of Py3NHCD and Im3NHCD are shown in Scheme 1. A common intermediate was 2,3-EpoCD,³⁰ whose hydroxyl groups were O-methylated by methyl iodide to produce 2,3-EpoPMeCD.²⁰ The $\text{S}_{\text{N}}2$ reactions of 2,3-EpoPMeCD with 3,5-bis(aminomethyl)pyridine and 3-(1*H*-imidazol-1-yl)pentane-1,5-diamine yielded Py3NHCD and Im3NHCD, respectively. In these reactions, epimerization occurs at the 2-position of the glucopyranose unit (Fig. 2). Therefore, the OH groups at the 2-positions of Py3NHCD and Im3NHCD take the axial configurations, while the other OCH₃ groups take the equatorial configurations. The linkers in Py3NHCD and Im3NHCD bind two cyclodextrin (CD) units with the –NH– linkages in the axial configurations at the 3- and 3'-positions of the CD units (Fig. 2).

One of the precursors of Im2CD is 2- N_3CD ,²⁹ which was prepared by the $\text{S}_{\text{N}}2$ reaction of 2-TsCD³¹ with the N_3^- anion (Scheme 2). In this reaction, the N_3 group at the 2-position of the glucopyranose unit takes an axial configuration. Because the following reactions do not induce epimerization, the two CD units



Scheme 2 Synthesis of Im2CD.

of Im2CD are linked to each other by amide bonds in axial configurations at the 2- and 2'-positions of the glucopyranose units (Fig. 2).

Complexation of cyclodextrin dimers with Fe^{III}TPPS

Fe^{III}TPPS exists as a μ -oxo-dimer ($\lambda_{\max} = 408$ nm) in aqueous solution at pH > 6.0.^{25,32–34} The pH titration curve provides an apparent pK_a of 6.6 for the equilibrium between the diaqua and μ -oxo dimer forms of Fe^{III}TPPS in aqueous solution (Fig. S1, ESI[†]).²¹ Upon the addition of Im2CD, Py3NHCD or Im3NHCD into the Fe^{III}TPPS solution at pH 8.0, the Soret band at 408 nm due to the μ -oxo-dimer shifted to 415–416 nm, which is attributed to the formation of a 1 : 1 inclusion complex of the CD dimer and Fe^{III}TPPS (Fig. S2–S4, ESI[†]). After the addition of equimolar amounts of Py3NHCD or Im2CD, the absorption spectral changes of Fe^{III}TPPS were sharply saturated, indicating the formation of very stable inclusion complexes. In the case of Im3NHCD, however, the absorbance change–porphyrin concentration profile could be analysed by an equation for a 1 : 1 inclusion complex formation to afford the binding constant (K) of 6.4×10^6 M⁻¹.

Acid dissociation of diprotonated TPPS/cyclodextrin dimer complexes

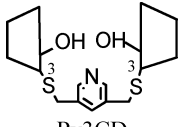
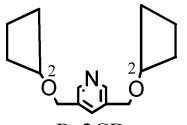
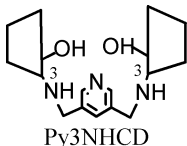
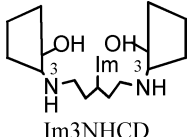
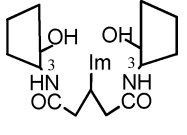
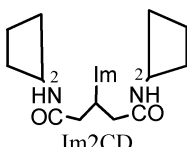
Two pyrrole nitrogen atoms of a free base porphyrin are protonated in an acidic solution. The apparent pK_a value of diprotonated tetrakis(4-sulfonatophenyl)porphyrin ($(H^+)_2$ TPPS) is 5.4 and this is lowered upon complexation with CDs.³⁵ The 2 : 1 inclusion complex of TPPS and heptakis(2,3,6-tri-*O*-methyl)- β -CD (TMe- β -CD) has a very low pK_a value (0.4), indicating that TMe- β -CD forms a very tight inclusion complex where two TMe- β -CD molecules encapsulate TPPS.³⁵ The pK_a value of TPPS can be used as a measure to know the extent of the encapsulation of

TPPS by two CD units. The pK_a values of $(H^+)_2$ TPPS encapsulated by Py3NHCD, Im3NHCD and Im2CD were measured. The results are summarized in Table 1 together with data from other CD dimers that have been studied previously. The pK_a values of $(H^+)_2$ TPPS bound to Py3NHCD and Im3NHCD were 3.2 and 3.1, respectively, and are much higher than that of the $(H^+)_2$ TPPS/TMe- β -CD complex (0.4). The most remarkable common feature of these two host molecules is the –NH– bonds at the bridge sites. Although we could not determine the pK_a values of these secondary amines experimentally, it is assumed that they must be higher than 9. Therefore, the –NH– groups at pH 7.0 must be protonated leading to a hydrophilic environment at the interspace of a capsule formed by the two CD units. Meanwhile, the pK_a value of the $(H^+)_2$ TPPS/Im2CD complex was 1.8, suggesting that the capsule formed by Im2CD was less hydrophilic than those of Py3NHCD and Im3NHCD, but more hydrophilic than those of Py3CD and Py2CD. The amide groups at the linker of Im2CD produce a wider interspace between the two CD units of its Fe^{III}TPPS inclusion complex because of the more rigid nature of the amide bonds.²³

Acid dissociation of the aqua complex of Fe^{III}TPPS bound to cyclodextrin dimers

The equilibrium between the diaqua ($\lambda_{\max} = 394$ nm) and μ -oxo dimer forms (408 nm), which corresponds to the equilibrium between the diaqua and hydroxo forms, can be observed by means of UV-vis spectroscopy. The apparent pK_a of $(H_2O)_2$ Fe^{III}TPPS in the absence of CD is 6.4.³⁶ The diaqua-mono hydroxo equilibrium ($pK_a = 4.3$) is directly observed when the ferric porphyrin is encapsulated by two TMe- β -CD molecules, which inhibit the formation of the μ -oxo-dimer.³⁶ Fe^{III}TPPS bound to Py3NHCD, Im3NHCD and Im2CD in an aqueous alkaline solution showed an absorption maximum at 415 nm, which is in good agreement with the λ_{\max} of (OH^-) Fe^{III}TPPS encapsulated by TMe- β -CD. As

Table 1 pK_a values of diprotonated TPPS ($(H^+)_2TPPS$) and monoanionic $Fe^{III}TPPS$ ($(H_2O)Fe^{III}TPPS$) complexed with various cyclodextrin dimers, $P_{1/2}$ values for formation of dioxygen adducts of $Fe^{II}TPPS$ /cyclodextrin dimer complexes and half-lives ($t_{1/2}$) of dioxygen adducts in phosphate buffer at pH 7

Dimer	pK_a of $(H^+)_2TPPS^a$	pK_a of $(H_2O)Fe^{III}TPPS^a$	$P_{1/2}/Torr^b$	$t_{1/2}/h$	Reference
 Py3CD	< 0.3	5.5	10 ± 0.5 (4 times)	30	20, 24
 Py2CD	< 0.3	6.9	176 ± 3 (3 times)	∞	22
 Py3NHCD	3.2	5.1	70 ± 5 (3 times)	1.3	this work
 Im3NHCD	3.1	6.8	1.5 ± 0.1 (4 times)	3.3	this work
 Im3CD	2.7	7.7	1.7	3.6	23
 Im2CD	1.8	7.4	36 ± 2 (5 times)	3.7	this work
H_2O	5.4	6.4	—	—	33, 35
TMe- β -CD	0.4	4.3	—	—	35, 36

^a The pK_a values were determined in 0.1 M $NaClO_4$ solution at 25 °C. The pH values were adjusted by aqueous NaOH and $HClO_4$. ^b The $P_{1/2}$ values were determined in phosphate buffer (0.05 M) at pH 7.0 and 25 °C.

the pH decreased, the λ_{max} shifted to 394 nm (Fig. S5–S7, ESI[†]), suggesting the formation of $(H_2O)Fe^{III}TPPS/CD$ dimer complexes where the axial nitrogenous ligands coordinate to the ferric centre of the porphyrin. The pK_a values of $(H_2O)Fe^{III}TPPS$ encapsulated by the CD dimers were evaluated by analysing the spectroscopic titration curves and the results are listed in Table 1 together with results previously reported for other CD dimer complexes. As shown in Table 1, the pK_a values of $(H_2O)Fe^{III}TPPS$ encapsulated by the CD dimers having an imidazole ligand are larger than those for the dimers having a pyridine ligand. The relatively high electron donating ability of the imidazole moiety destabilizes the $Fe^{III}-(OH^-)$ bond resulting in an increased pK_a value. Therefore, we may use pK_a as a measure to know the axial coordination bond strength of an imidazole complex. The pK_a value for the Im2CD complex (7.4) is slightly smaller than that for the Im3CD complex (7.7),

suggesting that the electron transfer from the axial ligand to the $Fe^{III}-(OH^-)$ bond occurs more effectively in the Im3CD complex than in the Im2CD complex. The pK_a value (6.8) of the $Fe^{III}TPPS$ complex of Im3NHCD is lower than those of Im3CD and Im2CD. However, the results for this complex cannot be directly compared to those for Im2CD and Im3CD because of the differences in the structures of their linkers. The two $-NH-$ groups at the linker of Im3NHCD are protonated and therefore an interspace between the two CD units of the $(H_2O)Fe^{III}TPPS/Im3NHCD$ complex provides favourable conditions for OH^- to remain. Microscopically high concentration of the hydroxide anion may lower the pK_a value of the $(H_2O)Fe^{III}TPPS/Im3NHCD$ complex.

On the other hand, the pK_a values of $(H_2O)Fe^{III}TPPS$ encapsulated by the CD dimers with pyridine linkers ($pK_a = 5.1$ – 6.9) are higher than that of the complex of TMe- β -CD (4.3).

(H₂O)₂Fe^{III}TPPS in a hydrophobic cage formed by the two TMe-β-CD molecules is unstable because of a positive charge at the centre of the ferric porphyrin, which tends to bind an OH⁻ anion to neutralize the charge. Though the two per-*O*-methylated β-CD units of Py3CD and Py2CD provide very hydrophobic environments around the porphyrin centre (*vide supra*), the p*K*_a values of (H₂O)Fe^{III}TPPS bound to these CD dimers are higher than that of the TMe-β-CD complex. The results can be interpreted in terms of the electron donating ability of the pyridine ligand, similar to the case of the imidazole ligand. The p*K*_a value for the Py2CD complex (6.9) is the largest amongst the Fe^{III}TPPS complexes with CD dimers having pyridine linkers. We have previously reported that the encapsulation of FeTPPS with Py2CD is so tight that a water molecule can barely penetrate the capsule.²² It is likely that the hydroxide anion also has difficulty in penetrating into the capsule, resulting in an increased p*K*_a even though (H₂O)Fe^{III}TPPS/Py2CD is unstable.

Formation and stabilities of the dioxygen adducts of Fe^{II}TPPS/CD dimer complexes

The formation of the dioxygen adducts of the Fe^{II}TPPS/CD dimer complexes was followed by UV-vis spectroscopy. We applied two methods to prepare the deoxy-, oxy- and CO-coordinated forms.

An excess amount of sodium dithionite (3–5 equiv. compared to Fe^{III}TPPS) was added to a mixture of Fe^{III}TPPS and a CD dimer (1.2 equiv.) in a de-aerated phosphate buffer (pH 7.0, 0.05 M). De-aeration of the phosphate buffer was performed by repeated freeze-pump-thaw-argon cycles. The stock solution of the Fe^{II}TPPS/CD dimer complex thus obtained was appropriately diluted using the same buffer, and the UV-vis spectrum of the deoxy-form was measured. O₂ gas was then gently introduced into the solution in a quartz cell to prepare an oxy-form of the Fe^{II}TPPS/CD dimer complex. In order to confirm the formation of the dioxygen adduct, whose spectrum is similar to that of the met-form, carbon monoxide (CO) gas was introduced into the oxygenated solution in the cell. If the O₂-adduct of the Fe^{II}TPPS/CD dimer complex was formed, a characteristically sharp absorption spectrum due to a CO-adduct of Fe^{II}TPPS would be observed. When the deoxy- and/or oxy-forms are autoxidized by O₂ to yield the met-form, no spectral change is observed upon the replacement of O₂ in the atmosphere with CO. As an example, the absorption spectral changes of the Fe^{II}TPPS/Im3NHCD complex during these procedures are shown in Fig. 3. The Soret band of the deoxy-form was observed at 433 nm that shifted to 422 nm under the O₂ atmosphere. The absorption spectrum changed again to show a characteristically sharp band centred at 423 nm, which is ascribed to the CO-adduct of the Fe^{II}TPPS/Im3NHCD complex, by changing the atmosphere from O₂ to CO. From these results, it can be concluded that the dioxygen adduct of the Fe^{II}TPPS/Im3NHCD complex is formed through the reaction of the Fe^{II}TPPS/Im3NHCD complex with O₂. However, this does not indicate the formation of the oxy-form in quantitative yield because of a possibility of partial autoxidation of the deoxy- and/or oxy-forms to the met-form whose absorption spectrum is similar to that of the oxy-form.

We then applied another procedure, which made it possible to accurately determine the extinction coefficients of the deoxy-, oxy- and CO-coordinated forms of the Fe^{II}TPPS complexes with CD

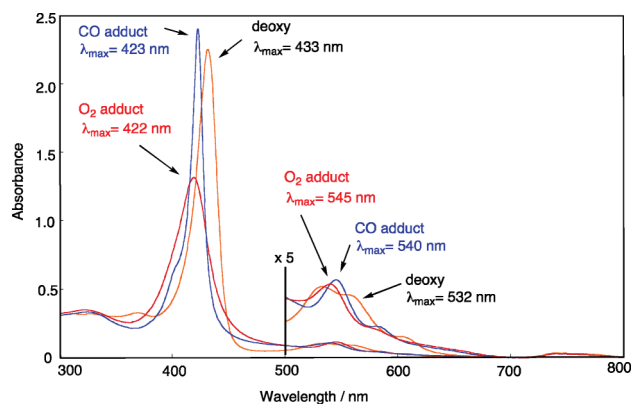


Fig. 3 UV-vis spectra of the Fe^{II}TPPS/Im3NHCD complex ([Fe^{II}TPPS] = 1.1 × 10⁻⁵ M, [Im3NHCD] = 1.3 × 10⁻⁵ M) under Ar, O₂, and CO atmospheres in 0.05 M phosphate buffer at pH 7.0 and 25 °C.

dimers and the yields of the oxy-forms in the oxygenation reactions of the deoxy forms. The extinction coefficients of the deoxy- (ϵ_{deoxy}) and CO-coordinated forms (ϵ_{CO}) of a Fe^{II}TPPS/CD dimer complex could be determined definitely in a phosphate buffer in the presence of an excess amount of Na₂S₂O₄. However, the extinction coefficient of the oxy-form could not be determined directly due to the autoxidation of the deoxy- and/or oxy-forms. The extinction coefficient of the oxy-form was determined as follows. First, the met-form of the FeTPPS/CD dimer complex in phosphate buffer (0.05 M, pH 7.0) was reduced using an excess amount of Na₂S₂O₄ and a solution of the deoxy-form was passed through a Sephadex G-25 desalting column to remove inorganic salts under aerobic conditions. The eluted solution was diluted with an O₂-saturated phosphate buffer to complete oxygenation. During this treatment, the deoxy-form completely disappeared. The UV-vis spectrum of the oxygenated solution was measured (Fig. 4, Spect. 1). After measuring the spectrum, the atmosphere in the quartz cell was replaced by CO, and the UV-vis spectrum of the CO-coordinated Fe^{II}TPPS/CD dimer complex was measured (Fig. 4, Spect. 2).

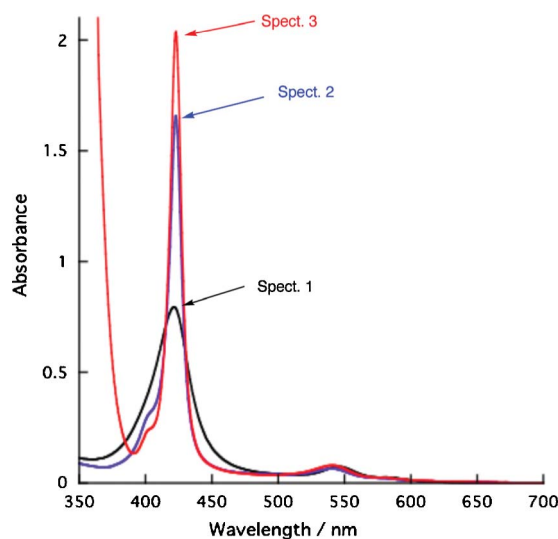


Fig. 4 UV-vis spectra of the products obtained by oxygenation of Fe^{II}TPPS/Im3NHCD complex (Spect. 1) and by carbonylation of the oxygenated product (Spect. 2 and 3). The experimental procedures are shown in the text.

Table 2 UV-vis spectral data of met-, deoxy-, oxy- and CO-coordinated forms of the FeTPPS/CD dimer complexes in phosphate buffer at pH 7.0 and 25 °C

host of FeTPPS	λ_{\max}/nm ($10^{-5} \epsilon/\text{M}^{-1}\text{cm}^{-1}$) of met-(OH) form	λ_{\max}/nm ($10^{-5} \epsilon/\text{M}^{-1}\text{cm}^{-1}$) of deoxy-form	λ_{\max}/nm ($10^{-5} \epsilon/\text{M}^{-1}\text{cm}^{-1}$) of oxy-form	λ_{\max}/nm ($10^{-5} \epsilon/\text{M}^{-1}\text{cm}^{-1}$) of CO-form
Py3CD	418 (1.19)	434 (2.13)	423 (1.64)	422 (3.71)
Py2CD	410 (1.13)	434 (2.26)	422 (1.55)	422 (3.61)
Py3NHCD	416 (1.22)	431 (2.41)	420 (1.38)	422 (3.65)
Im3CD	414 (1.27)	434 (2.25)	423 (1.74)	424 (3.89)
Im2CD	412 (1.17)	435 (2.67)	424 (1.59)	424 (3.73)
Im3NHCD	414 (1.33)	433 (2.09)	422 (1.69)	423 (3.89)

After this, an excess amount of $\text{Na}_2\text{S}_2\text{O}_4$ was further added to the solution under the CO atmosphere and the UV-vis spectrum was measured again (Fig. 4, Spect. 3). A_{oxy} , A_{COa} and A_{COb} are the absorbances at λ_{\max} (Soret bands) of Spect. 1, Spect. 2 and Spect. 3, respectively.

The total concentration of FeTPPS (C_{total}) is represented by

$$C_{\text{total}} = A_{\text{COb}}/\epsilon_{\text{CO}} \quad (1)$$

where A_{COa} is the sum of the absorbances of the CO-adduct and the met-form:

$$A_{\text{COa}} = \epsilon_{\text{CO}}C_{\text{CO}} + \epsilon_{\text{met}}C_{\text{met}} \quad (2)$$

where ϵ_{met} is the extinction coefficient of the met-form, and C_{CO} and C_{met} are the concentrations of the CO-adduct and the met-form, respectively, in the oxygenated solution. C_{total} can be represented by eqn (3).

$$C_{\text{total}} = C_{\text{CO}} + C_{\text{met}} \quad (3)$$

Eqn (4) can be derived from eqn (2) and (3).

$$C_{\text{CO}} = (A_{\text{COa}} - \epsilon_{\text{met}}C_{\text{total}})/(\epsilon_{\text{CO}} - \epsilon_{\text{met}}) \quad (4)$$

It is reasonable to assume that C_{CO} corresponds to the concentration of the oxy-form (C_{oxy}) in the oxygenated sample. The ratio of $\text{Fe(II)}/[\text{Fe(II)} + \text{Fe(III)}]$ of the sample shown in Spect. 2 is given in eqn (5).

$$\text{Fe(II)}/[\text{Fe(II)} + \text{Fe(III)}] = C_{\text{CO}}/C_{\text{total}} = C_{\text{oxy}}/C_{\text{total}} \quad (5)$$

Because C_{total} and C_{CO} can be determined from eqn (1) and (4), respectively, the contents of the oxy- and met-forms in the oxygenated sample (Fig. 4, Spect. 1) can be evaluated from eqn (5). A_{oxy} in Spect. 1 is expressed as:

$$A_{\text{oxy}} = \epsilon_{\text{oxy}}C_{\text{oxy}} + \epsilon_{\text{met}}C_{\text{met}} \quad (6)$$

C_{oxy} and C_{met} can be obtained from eqn (1), (4) and (5), and therefore the extinction coefficient of the oxy-form (ϵ_{oxy}) can be determined from eqn (6).

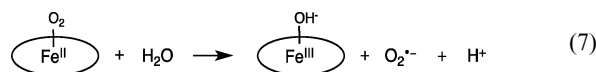
The spectroscopic data of the met-, deoxy-, oxy- and CO-coordinated forms of the FeTPPS/CD dimer complexes are summarized in Table 2. Because Fe^{III} TPPS is a hygroscopic material, its concentration was determined from the reported ϵ_{met} value ($1.52 \times 10^5 \text{ M}^{-1}\text{cm}^{-1}$ at 392 nm).²⁵ A series of spectroscopic measurements also informed us of the extent of autoxidation that occurred during the oxygenating process of a deoxy-form, which included treatment with a Sephadex G25 column under aerobic conditions. The yields of the oxy-forms after these procedures could be evaluated from C_{total} and C_{oxy} and the results are summarized in Table 3, which indicates that a considerable amount

Table 3 Yields of the oxy-forms in oxygenation reactions of the Fe^{II} TPPS/CD dimer complexes that occurred during Sephadex G25 column chromatography under aerobic conditions at pH 7.0 and 25 °C

Host of FeTPPS	Yield of O_2 - Fe^{II} TPPS/ CD dimer complex/%	$t_{1/2}/\text{h}$
Py3CD	75	30
Py2CD	85	∞
Py3NHCD	58	1.3
Im3CD	69	3.6
Im2CD	80	3.7
Im3NHCD	75	3.3

of the met-form is simultaneously recovered in the oxygenation reaction of each deoxy complex. We are empirically aware that the oxy-forms of the Fe^{II} TPPS/CD dimer complexes are easily autoxidized by mechanical shaking.

The autoxidation rates of the dioxygen adducts of the Fe^{II} TPPS complexes of Py3NHCD, Im3NHCD and Im2CD to their met-forms were followed by monitoring their progressive absorbance changes (Fig. S8, ESI†). In each case, the oxy-form was converted to the met-form according to first-order kinetics, and no degradation of the porphyrin ring was observed. The half-lives ($t_{1/2} = \ln 2/k_{\text{obs}}$) of the dioxygen adducts are listed in Table 1. As previously reported, the dioxygen adducts of the Fe^{II} TPPS complexes with Py3CD ($t_{1/2} = 30 \text{ h}$) and Py2CD (∞) are extremely stable. Meanwhile, the O_2 adducts of other CD dimers were considerably unstable (1.3–3.7 h). Shikama and co-workers proposed a mechanism for the autoxidation of the dioxygen adducts of heme proteins that involves the nucleophilic attack of a water molecule to the $\text{Fe}^{\text{II}}\text{-O}_2$ bond to generate Fe^{III} and a superoxide ion.³⁷ We also reported the H_2O - and inorganic anion-promoted autoxidation of the dioxygen adduct of the Fe^{II} TPPS/Py3CD complex (eqn (7)):²¹



If the O_2 adduct of a receptor has a short $t_{1/2}$, the Fe(II) centre of the receptor may be located in a hydrophilic environment where water molecules can easily penetrate. The stabilities of the O_2 adducts correlate with the hydrophilicity at the CD interspaces evaluated from the $\text{p}K_{\text{a}}$ values of the $(\text{H}^+)_{2}\text{TPPS}$ complexes with the CD dimers. The O_2 receptors having hydrophilic interspaces between the two CD units had the short $t_{1/2}$ values. The rigid amide bonds at the linker positions of Im2CD and Im3CD seem to expand the interspaces leading to a hydrophilic environment around the Fe(II) centre of the Fe^{II} TPPS complexes of these CD dimers. Meanwhile, Py3NHCD and Im3NHCD may also form the

hydrophilic interspaces of the capsules because of the protonation to the $-\text{NH}-$ bonds of these CD dimers.

Dioxygen affinities of Fe^{II} TPPS/CD dimer complexes

The dioxygen affinities of the Fe^{II} TPPS/CD dimer supramolecular complexes were evaluated from $P_{1/2}$ values. The $P_{1/2}$ values were determined by monitoring the changes in absorbance due to a deoxy-form (ΔA) of the iron porphyrin under various dioxygen pressures (P^{O_2}) diluted by pure N_2 (Fig. 5). $P_{1/2}$ can be correlated with P^{O_2} and ΔA as represented in eqn (8);³⁸

$$P^{\text{O}_2} = (\Delta\epsilon[\text{Fe}^{\text{II}}\text{TPPS/CD dimer}]_t, P^{\text{O}_2}) / \Delta A - P_{1/2} \quad (8)$$

where $\Delta\epsilon$ is the difference in the extinction coefficients between the deoxy- and oxy-forms at a given wavelength. The intercept of a straight line between $P^{\text{O}_2} / \Delta A$ and P^{O_2} corresponds with $P_{1/2}$ (inset of Fig. 5). The stock solutions of the deoxy forms were prepared by removing inorganic salts using a Sephadex G25 column and

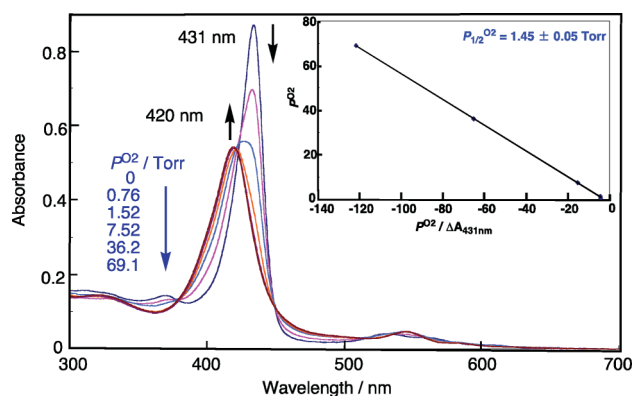


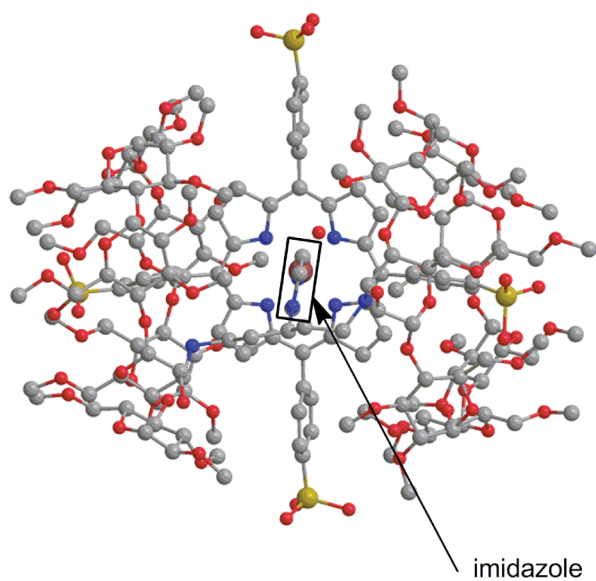
Fig. 5 UV-vis spectral changes of Fe^{II} TPPS/Im3NHCD ($[\text{Fe}^{\text{II}}\text{TPPS}] = 5.0 \times 10^{-6}$ M, $[\text{Im3NHCD}] = 6.0 \times 10^{-6}$ M) as a function of the O_2 partial pressure (P^{O_2}) in N_2 in 0.05 M phosphate buffer at pH 7.0 and 25 °C.

stored at a low temperature (*ca.* 5 °C). The autoxidation of the oxy-forms was markedly depressed at low temperature.

The $P_{1/2}$ values thus obtained for the Fe^{II} TPPS complexes with Py3NHCD, Im3NHCD and Im2CD are listed in Table 1 together with those for other systems that have been reported previously. The Fe^{II} TPPS/Im3NHCD complex showed a high O_2 affinity ($P_{1/2} = 1.5 \pm 0.1$ Torr), similar to that of the Fe^{II} TPPS/Im3CD complex (1.7 Torr).²³ The position of the linkers of the CD dimers and the proximal ligand are similar between these two complexes showing high O_2 affinities. Both CD dimers have linkers in axial positions on the 3- and 3'-positions of the glucopyranose units. Although Im2CD has an imidazole ligand, its Fe^{II} TPPS complex shows an intermediate O_2 affinity (36 ± 2 Torr). Two of the CD units of Im2CD are connected by a linker in axial configurations at the 2- and 2'-positions. Therefore, the structures of the Fe^{II} TPPS complexes with Im3NHCD and Im3CD should be different from that of the Im2CD complex (*vide infra*).

We have the data about three complexes whose linkers involve the pyridine ligand. The receptor showing the smallest O_2 affinity ($P_{1/2} = 176 \pm 3$ Torr) is hemoCD2, of which the pyridine linker is connected at the 2- and 2'-positions of the cyclodextrin units, while the receptors having the pyridine linkers at the 3- and 3'-positions show intermediate $P_{1/2}$ values (10 ± 0.5 and 70 ± 5 Torr for hemoCD1 and Fe^{II} TPPS/Py3NHCD, respectively). The steric constraint of a receptor having a nitrogenous axial ligand at the 2- and 2'-positions of the cyclodextrin units may elongate a ligand-Fe bond distance to weaken the electron transfer from the ligand to $\text{Fe}(\text{II})$. To confirm such an assumption, we need to have data of X-ray and/or detailed NMR analysis. Because we have not been able to determine any of the supramolecular receptors' structures, we calculated the energy-minimized structures of the dioxygen adducts of the Fe^{II} TPPS complexes of Py2CD and Im3NHCD that show the largest and smallest $P_{1/2}$ values, respectively. The structures calculated using a Conflex/MM3 (extensive) method are shown in Fig. 6 (pdb files, ESI[†]), which suggests a complete

O_2 - $\text{Fe}(\text{II})$ TPPS/Im3NHCD



O_2 -hemoCD2

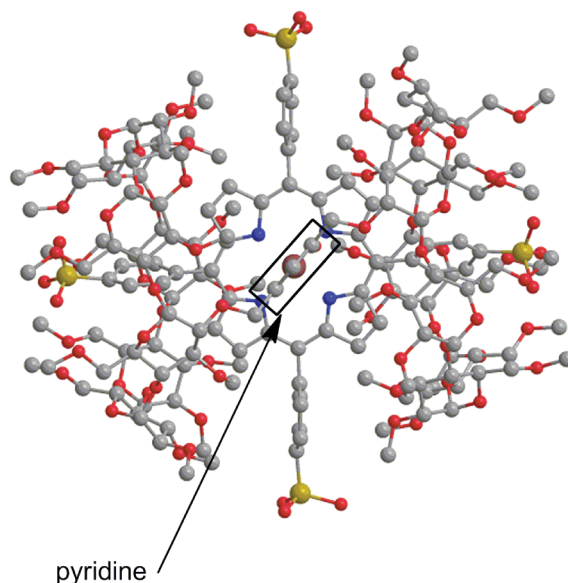


Fig. 6 Energy-minimized structures of the dioxygen adducts of the Fe^{II} TPPS complexes of Im3NHCD and Py2CD. The structures were obtained from the Conflex/MM3 (extensive) calculations.

eclipsed orientation of the axial ligand for the Py2CD complex and the staggered orientation for the Im3NHCD complexes. Although there is no assurance that the Coflex/MM3 calculation provides a real structure of a supramolecular receptor, it suggests a possibility that steric hindrance between the axial ligand and the pyrrole nitrogen affects a ligand–Fe(II) distance to control the dioxygen affinity.

Conclusions

The present and previous studies on supramolecular Hb/Mb models make it possible to design a globin model in which the Fe^{II}TPPS moiety shows a desirable dioxygen affinity. We are trying to synthesise such a supramolecule. “The higher O₂ affinity, the better O₂ receptor” is not always right. It is important to prepare a dioxygen receptor whose O₂ affinity is just appropriate for a purpose. We prepared various O₂ receptors having *P*_{1/2} values from 1.5 to 176 Torr.

Acknowledgements

This study was supported by Grants-in-Aid on Scientific Research B (no. 21350097) and “Creating Research Center for Advanced Molecular Biochemistry”, Strategic Development of Research Infrastructure for Private Universities from the Ministry of Education, Culture, Sports, Science and Technology (Japan).

References

- 1 B. A. Springer, S. G. Sligar, J. S. Olson and G. N. Phillips Jr., *Chem. Rev.*, 1994, **94**, 699–714.
- 2 M. Momenteau and C. A. Reed, *Chem. Rev.*, 1994, **94**, 659–698.
- 3 J. A. Lukin and C. Ho, *Chem. Rev.*, 2004, **104**, 1219–1230.
- 4 G. K. Ackers and J. M. Holt, *J. Biol. Chem.*, 2006, **281**, 11441–11443.
- 5 T. Yonetani and M. Labergue, *Biochim. Biophys. Acta, Proteins Proteomics*, 2008, **1784**, 1146–1158.
- 6 J. B. Wittenberg, F. J. Bergeson, C. A. Appleby and G. L. Turner, *J. Biol. Chem.*, 1974, **249**, 4057–4066.
- 7 M. L. Quilline, R. M. Arduini, J. S. Olson and G. N. Phillips, Jr., *J. Mol. Biol.*, 1993, **234**, 140–155.
- 8 M. S. Hargrove, J. K. Barry, E. A. Brucker, M. B. Berry, G. N. Phillips, Jr., J. S. Olson, R. Arredondo-Peter, J. M. Dean, R. V. Klucas and G. Sarath, *J. Mol. Biol.*, 1997, **266**, 1032–1042.
- 9 S. S. Narula, C. Dalvit, C. A. Appleby and P. E. Wright, *Eur. J. Biochem.*, 1988, **178**, 419–435.
- 10 Q. H. Gibson, J. B. Wittenberg, B. A. Wittenberg, D. Bogusz and C. A. Appleby, *J. Biol. Chem.*, 1989, **264**, 100–107.
- 11 D. Barrick, *Biochemistry*, 1994, **33**, 6546–6554.
- 12 E. H. Harutyunyan, T. N. Safonova, I. P. Kuranova, A. N. Popov, A. A. Teplyakov, B. K. Vainshtein, G. G. Dodson, J. C. Wilson and M. F. Perutz, *J. Mol. Biol.*, 1995, **251**, 104–115.
- 13 S. Kundu, B. Snyder, K. Das, P. Chowdhury, J. Park, J. W. Petrich and M. S. Hargrove, *Proteins: Struct., Funct., Genet.*, 2002, **46**, 268–277.
- 14 L. Capece, M. A. Marti, A. Crespo, F. Doctorovich and D. A. Estrin, *J. Am. Chem. Soc.*, 2006, **128**, 12455–12461.
- 15 J. P. Collman, R. Boulatov, C. J. Sunderland and L. Fu, *Chem. Rev.*, 2004, **104**, 561–588.
- 16 J. S. Olson, A. J. Mathews, R. J. Rohlf, B. A. Springer, A. Barry, K. D. Egeberg, S. G. Sligar, J. Tame, J. P. Renaud, P. Jean and K. Nagai, *Nature (London)*, 1988, **336**, 265–266.
- 17 E. E. Scott, Q. H. Gibson and J. S. Olson, *J. Biol. Chem.*, 2001, **276**, 5177–5188.
- 18 I. Birukou, R. L. Schweers and J. S. Olson, *J. Biol. Chem.*, 2010, **285**, 8840–8854.
- 19 T. Suzuki, Y. Watanabe, M. Nagasawa, A. Matsuoka and K. Shikama, *Eur. J. Biochem.*, 2000, **267**, 6166–6174.
- 20 K. Kano, H. Kitagishi, M. Kodera and S. Hirota, *Angew. Chem., Int. Ed.*, 2005, **44**, 435–438.
- 21 K. Kano, H. Kitagishi, C. Dagallier, M. Kodera, T. Matsuo, T. Hayashi, Y. Hisaeda and S. Hirota, *Inorg. Chem.*, 2006, **45**, 4448–4460.
- 22 K. Kano, Y. Itoh, H. Kitagishi, T. Hayashi and S. Hirota, *J. Am. Chem. Soc.*, 2008, **130**, 8006–8015.
- 23 K. Kano, H. Kitagishi, T. Mabuchi, M. Kodera and S. Hirota, *Chem.–Asian J.*, 2006, **3**, 358–366.
- 24 K. Kano, T. Ochi, S. Okunaka, Y. Ota, K. Karasugi, T. Ueda and H. Kitagishi, *Chem. Asian J.*, DOI: 10.1002/asia.201100354.
- 25 E. B. Fleischer, J. M. Palmer, T. S. Srivastava and A. Chatterjee, *J. Am. Chem. Soc.*, 1971, **93**, 3162–3167.
- 26 M.-C. Lagunas, R. A. Gossage, W. J. J. Smeets, A. L. Spek and G. van Koten, *Eur. J. Inorg. Chem.*, 1998, 163–168.
- 27 L.-Y. Kong, H.-F. Zhu, T. Okamura, Y.-H. Mei, W.-Y. Sun and N. Ueyama, *J. Inorg. Biochem.*, 2006, **100**, 1272–1279.
- 28 S. Gil, P. Zaderenzo, F. Cruz, S. Cerdán and P. Ballesteros, *Bioorg. Med. Chem.*, 1994, **2**, 305–314.
- 29 Y.-F. Poon, I. W. Muderawan and S.-C. Ng, *J. Chromatogr., A*, 2006, **1101**, 185–197.
- 30 R. Breslow, A. W. Czarnik, M. Lauer, R. Leppkes, J. Winkler and S. Zimmerman, *J. Am. Chem. Soc.*, 1986, **108**, 1969–1979.
- 31 H. Yu, A. Teramoto, M. Fukudome, R.-G. Xie, D.-Q. Yuan and K. Fujita, *Tetrahedron Lett.*, 2006, **46**, 8837–8840.
- 32 K. Hatano and Y. Ishida, *Bull. Chem. Soc. Jpn.*, 1982, **55**, 3333–3334.
- 33 S. Mosseri, J. C. Mialocq, B. Perly and P. Hambright, *J. Phys. Chem.*, 1991, **95**, 4659–4663.
- 34 S. C. M. Gandini, V. E. Yushmanov and M. Tabak, *J. Bioinorg. Chem.*, 2001, **85**, 263–277.
- 35 K. Kano, N. Tanaka, H. Minamizono and Y. Kawakita, *Chem. Lett.*, **1996**, 925–926.
- 36 K. Kano, H. Kitagishi, S. Tamura and A. Yamada, *J. Am. Chem. Soc.*, 2004, **126**, 15202–15210.
- 37 K. Shikama, *Chem. Rev.*, 1998, **98**, 1357–1373.
- 38 A. Zingg, B. Felber, V. Gramlich, L. Fu, J. P. Collman and F. Diederich, *Helv. Chim. Acta*, 2002, **85**, 333–351.